*Supplementary Information for：*

**Mechanisms insight into oxygen reduction reaction on the dual FeN$_2$ embedded graphene for**

**proton exchange membrane fuel cells**

Wenjie Qi[a,b,d, e], Xianming Zhang[b], Juntian Niu[c*], Zhigang Zhang[a*], Jiale Huang[a], Shuaishuai Ge[a], Yi

Zhang[a]

[a] Key Laboratory of Advanced Manufacturing Technology for Automobile Parts, Ministry of

Education, Chongqing University of Technology, Chongqing 400050, China

[b] Engineering Research Center for Waste Oil Recovery Technology and Equipment, Ministry of

Education, Chongqing Technology and Business University, Chongqing 400067, China

[c] College of Electrical and Power Engineering, Taiyuan University of Technology, Taiyuan, Shanxi,

030024, China

[d] Department of Chemistry, Fujian Province University Key Laboratory of Green Energy and

Environment Catalysis, Ningde Normal University, Ningde, 352100, China

[e] Key Laboratory of Low-grade Energy Utilization Technologies and Systems, Ministry of Education

of PRC, Chongqing University, Chongqing 400044, China

*Corresponding authors: Juntian Niu, Zhigang Zhang

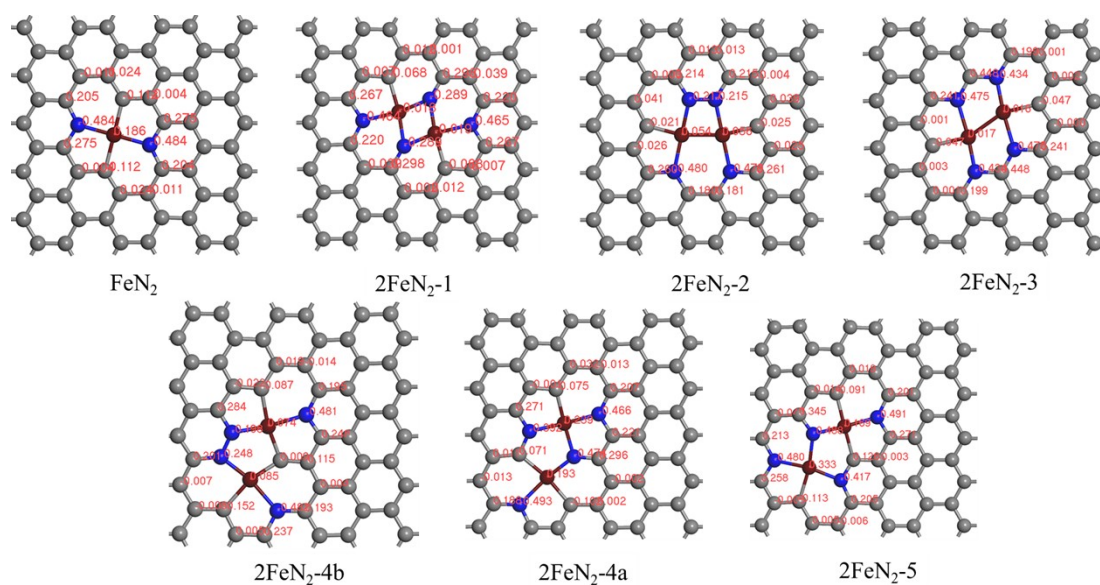E-mail: juntianniu@163.com; zhangzhigang@cqut.edu.cn
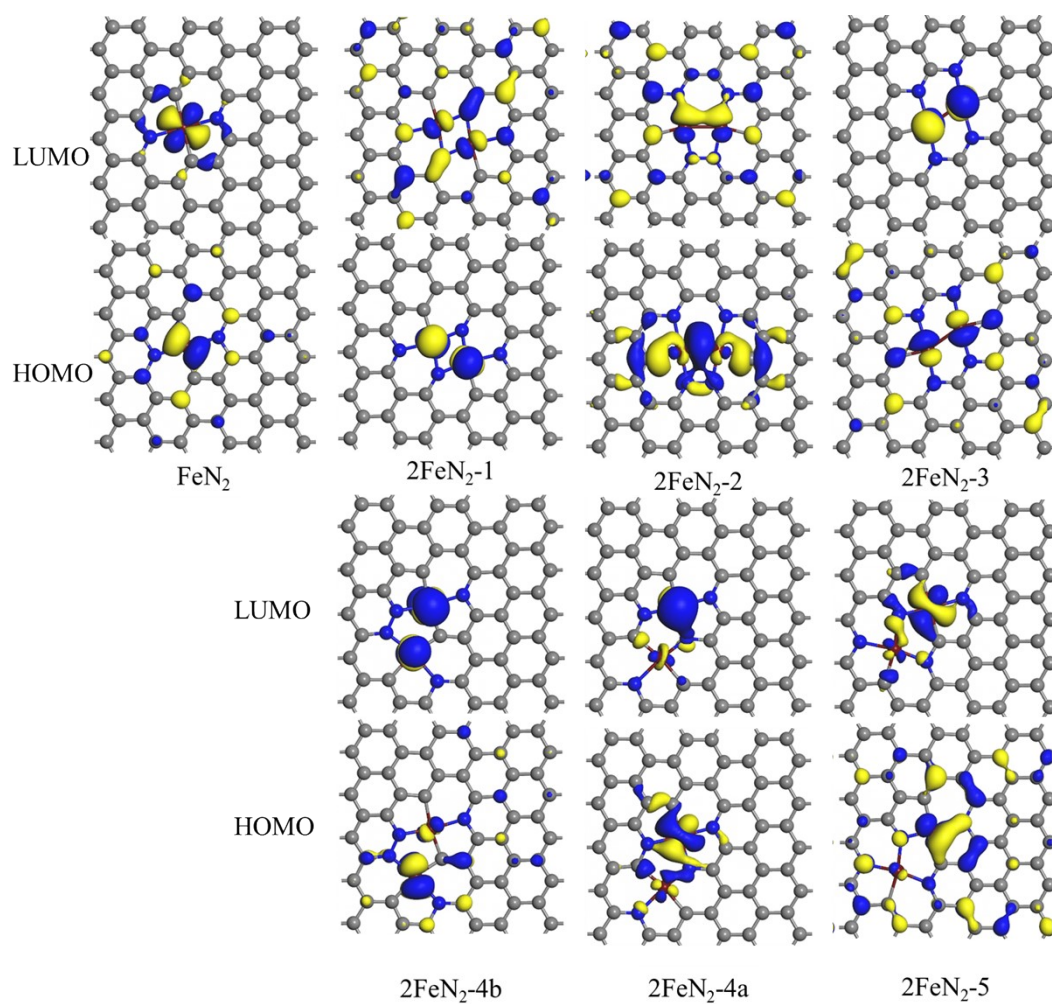
Fig. S1. Mulliken charges of these catalysts.



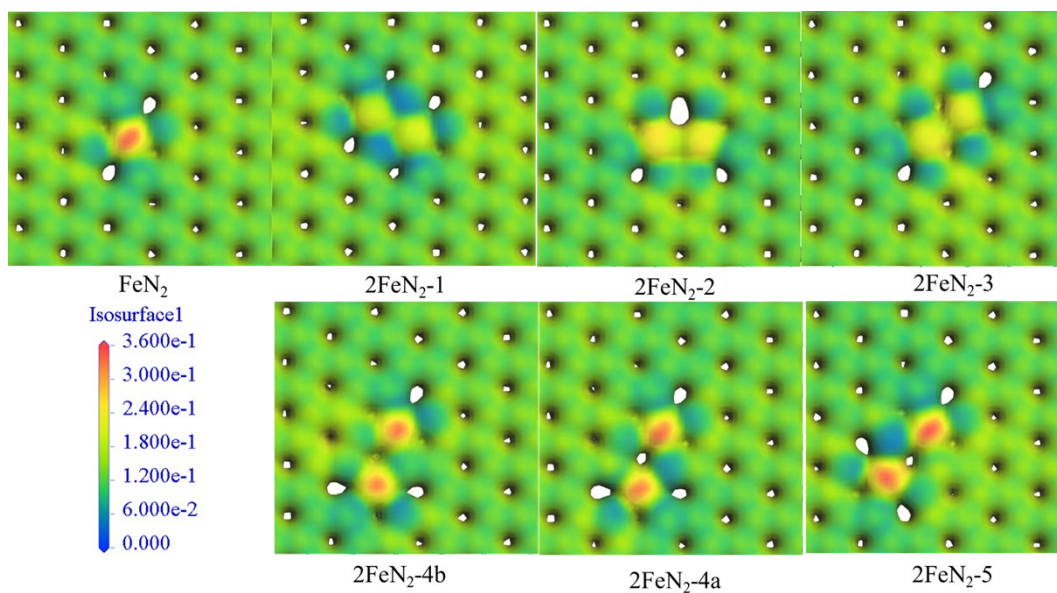Fig. S2. HOMO and LUMO of these catalysts.

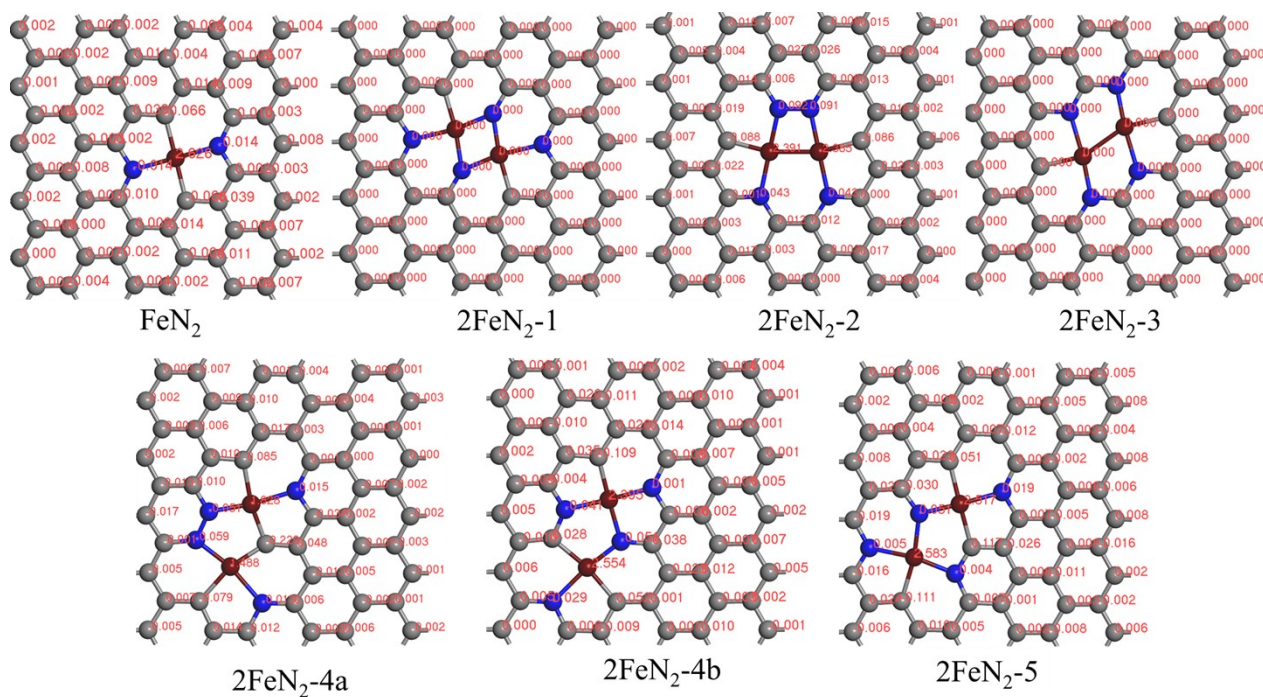Fig. S3. the electrostatic potential surface of these catalysts.



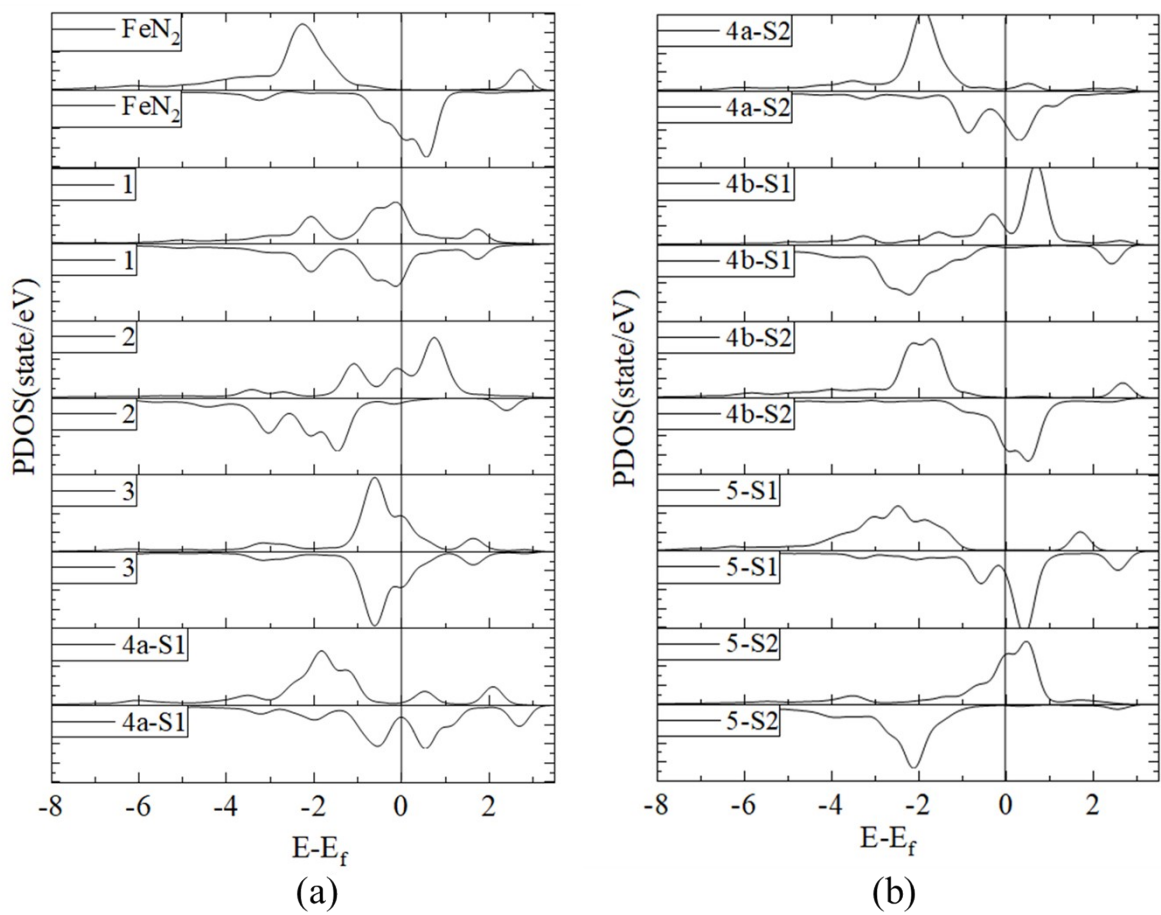Fig. S4. The magnetic moments on Fe atom of these catalysts.

Fig.S5. PDOS for the Fe atom of these catalysts, the value of the PDOS varies in a range of -3.3 eV to 3.3 eV.
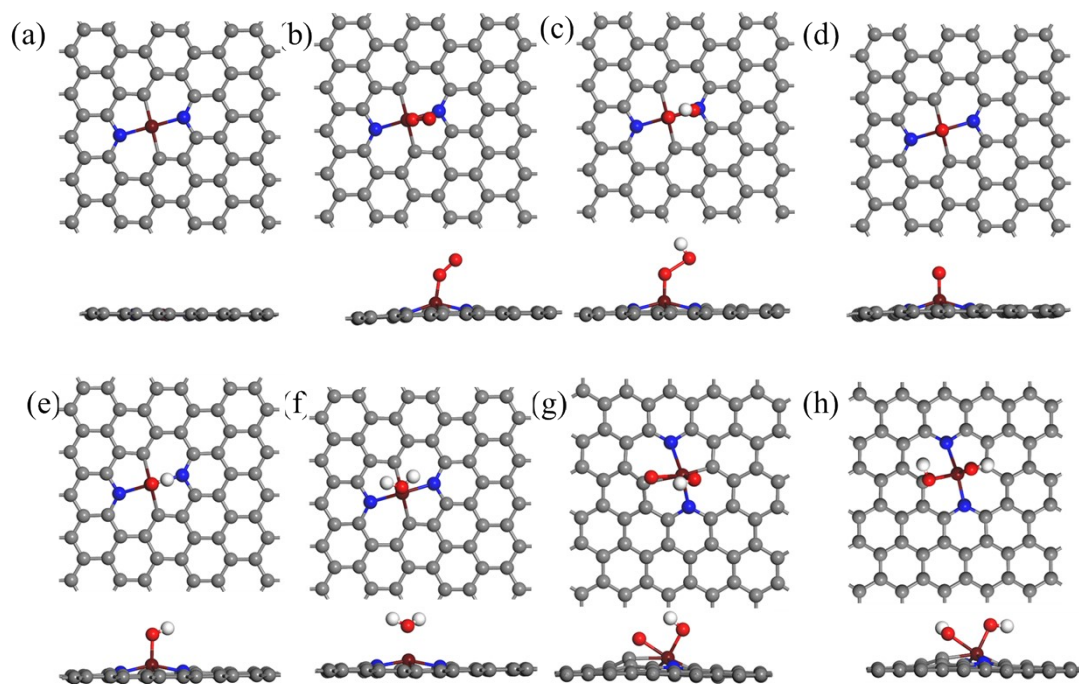
Fig. S6 Optimal structures of the oxygen-containing intermediates adsorbed on FeN$_2$/G catalytic surface. (a)*, (b) *O$_2$, (c) *OOH, (d) *O, (e) *OH, (f)H$_2$O*, (g) *O+*OH, (h) *OH+*OH.

====================================================================================



Fig. S7 Optimal structures of the oxygen-containing intermediates adsorbed on Fe$_2$N$_4$-1/G catalytic surface. (a)*, (b) *O$_2$, (c) *OOH, (d) *O, (e) *OH, (f)H$_2$O*, (g) *O+*OH, (h) *OH+*OH.
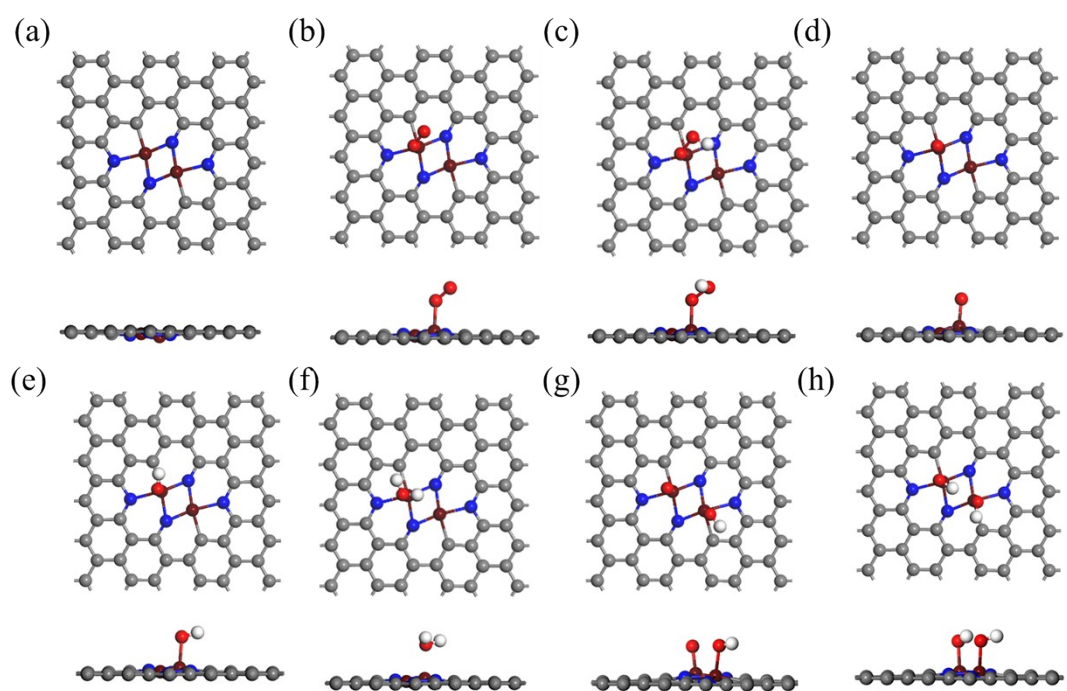
Fig. S8 Optimal structures of the oxygen-containing intermediates adsorbed on $Fe_2N_4$-2/G catalytic surface. (a)*, (b) $*O_2$, (c) *OOH, (d) *O, (e) *OH, (f)$H_2O$*, (g) *O+*OH, (h) *OH+*OH.

===========================================================================================



Fig. S9 Optimal structures of the oxygen-containing intermediates adsorbed on $Fe_2N_4$-3/G catalytic surface. (a)*, (b) $*O_2$, (c) *OOH, (d) *O, (e) *OH, (f)$H_2O$*, (g) *O+*OH, (h) *OH+*OH.
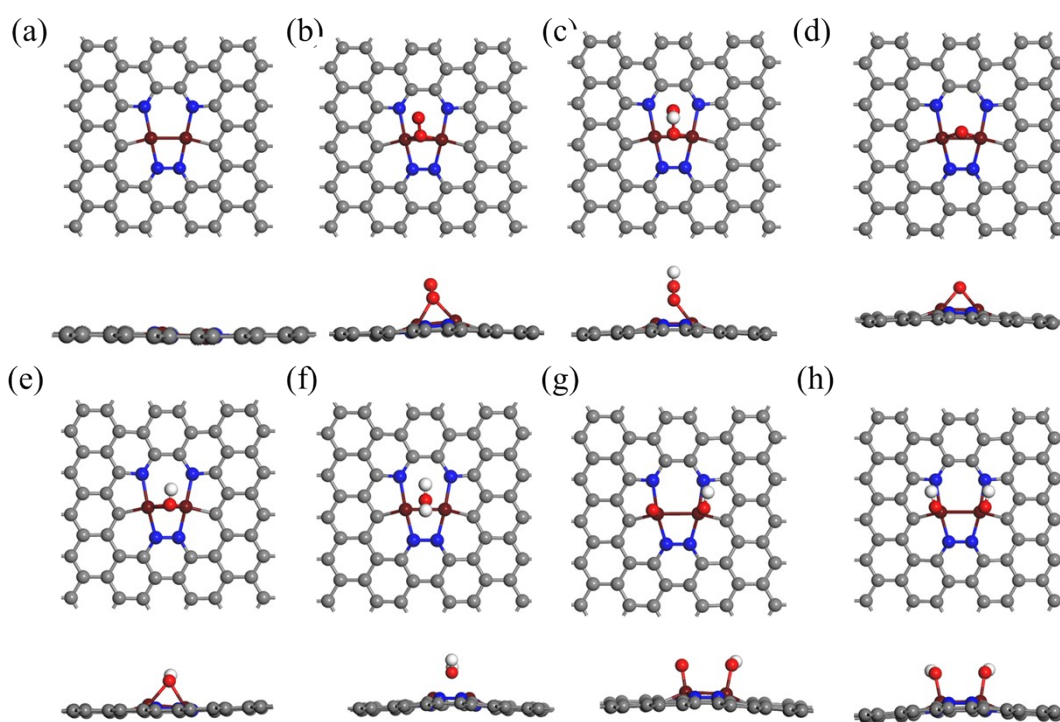
Fig. S10 Optimal structures of the oxygen-containing intermediates adsorbed on $Fe_2N_4$-4a-S1/G catalytic surface. (a)*, (b) *$O_2$, (c) *OOH, (d) *O, (e) *OH, (f)$H_2O$*, (g) *O+*OH, (h) *OH+*OH.
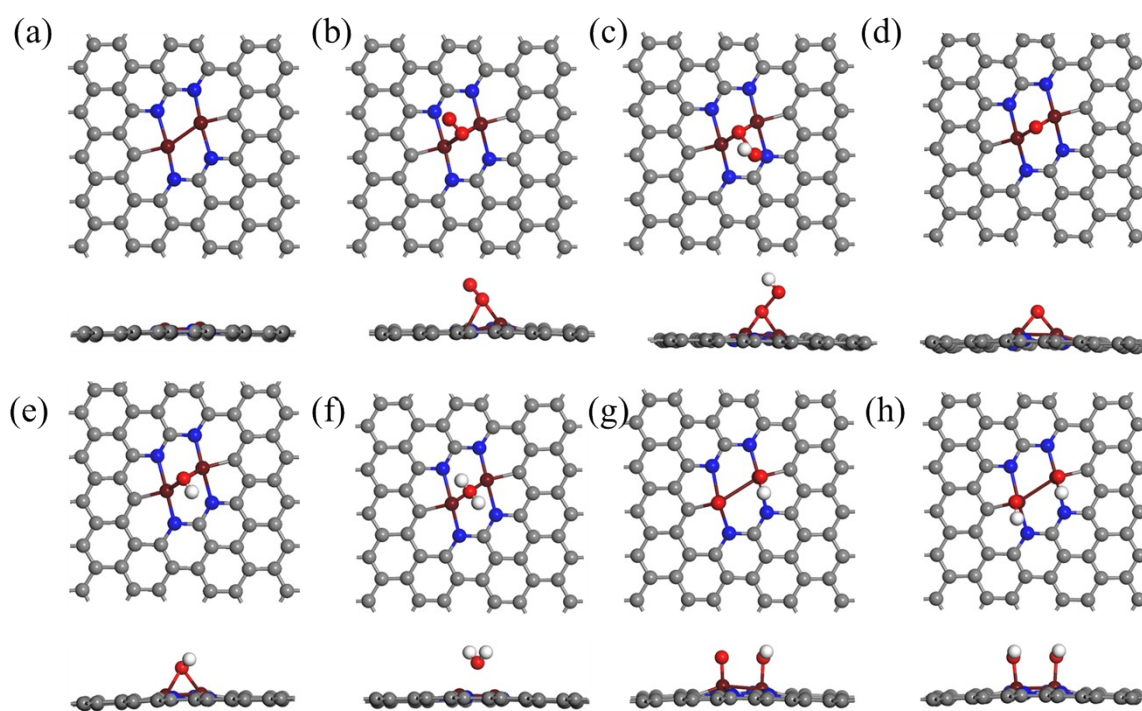


Fig. S11 Optimal structures of the oxygen-containing intermediates adsorbed on $Fe_2N_4$-4a-S2/G catalytic surface. (a)*, (b) *$O_2$, (c) *OOH, (d) *O, (e) *OH, (f)$H_2O$*, (g) *O+*OH, (h) *OH+*OH.

Fig. S12 Optimal structures of the oxygen-containing intermediates adsorbed on $Fe_2N_4$-4b-S1/G catalytic surface. (a)*, (b) *$O_2$, (c) *OOH, (d) *O, (e) *OH, (f)$H_2O$*, (g) *O+*OH, (h) *OH+*OH.
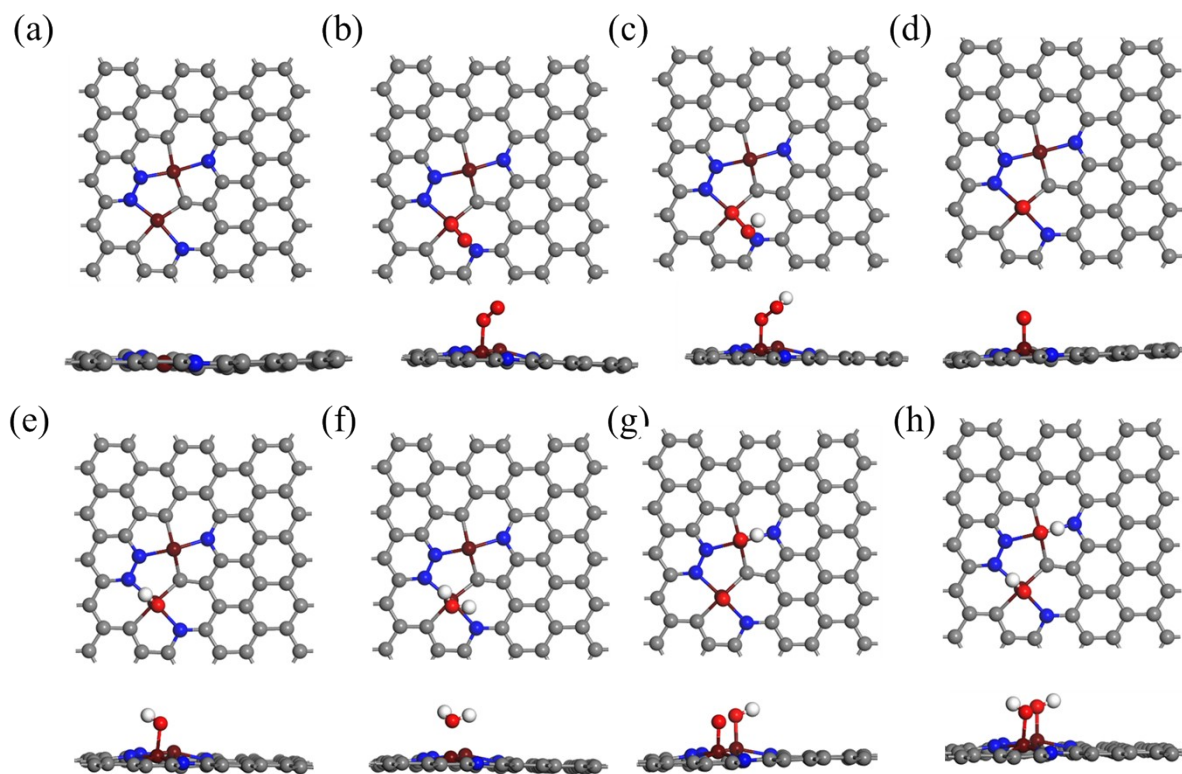


Fig. S13 Optimal structures of the oxygen-containing intermediates adsorbed on $Fe_2N_4$-4b-S2/G catalytic surface. (a)*, (b) *$O_2$, (c) *OOH, (d) *O, (e) *OH, (f)$H_2O$*, (g) *O+*OH, (h) *OH+*OH.
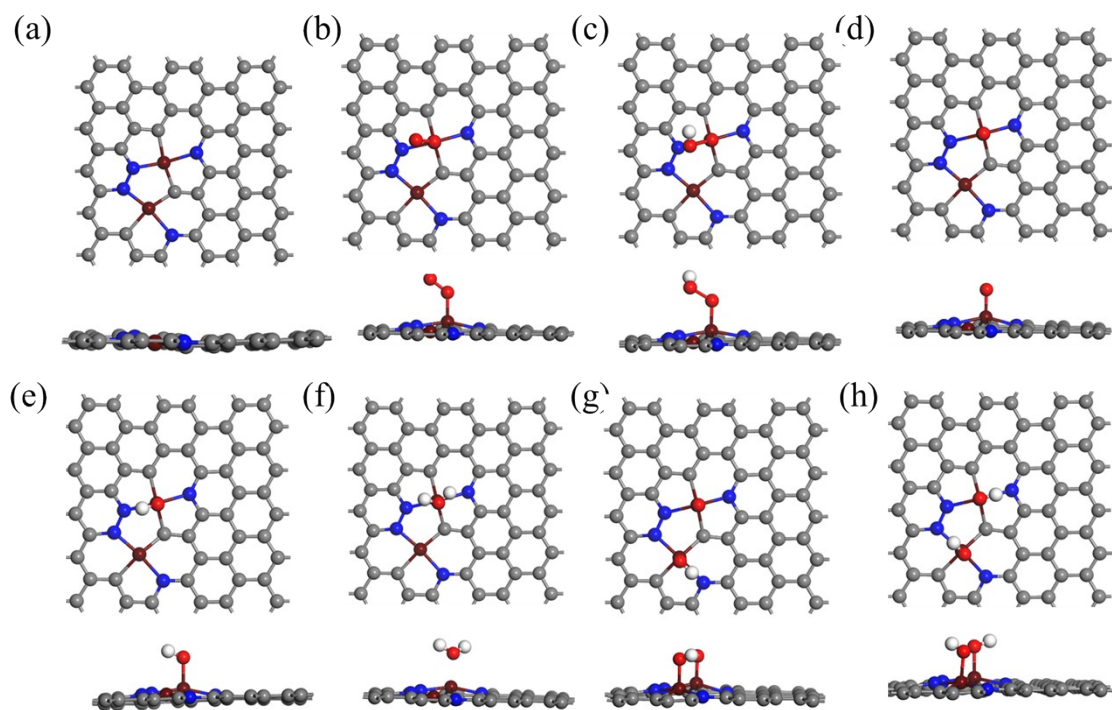
Fig. S14 Optimal structures of the oxygen-containing intermediates adsorbed on $Fe_2N_4$-5-S1/G catalytic surface. (a)*, (b) *$O_2$, (c) *OOH, (d) *O, (e) *OH, (f)$H_2O$*, (g) *O+*OH, (h) *OH+*OH.

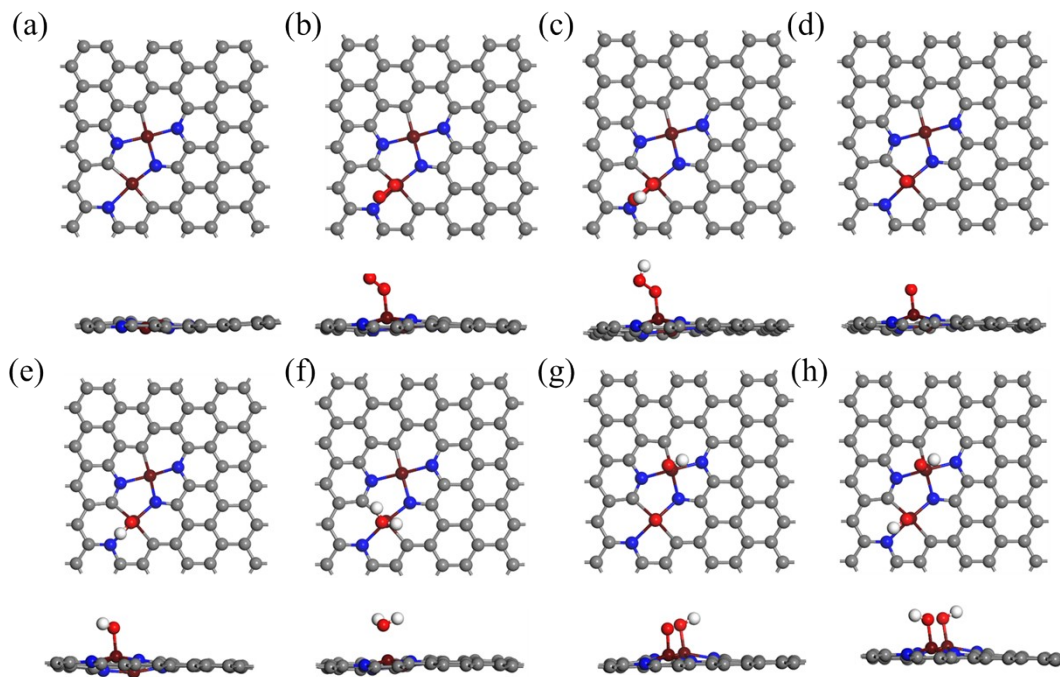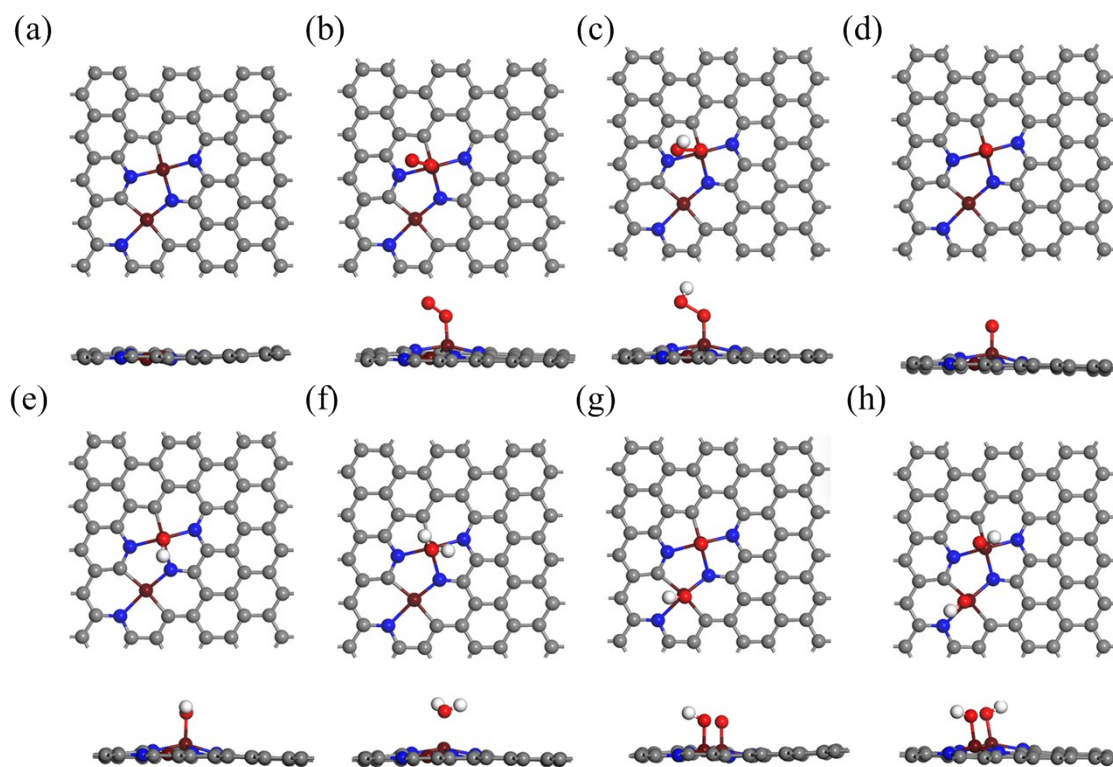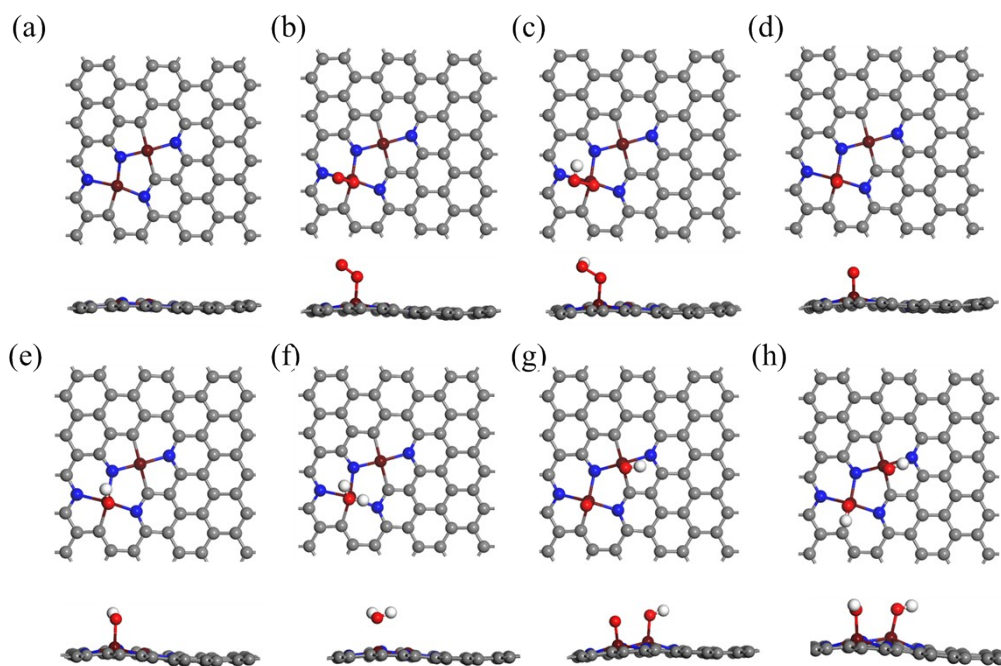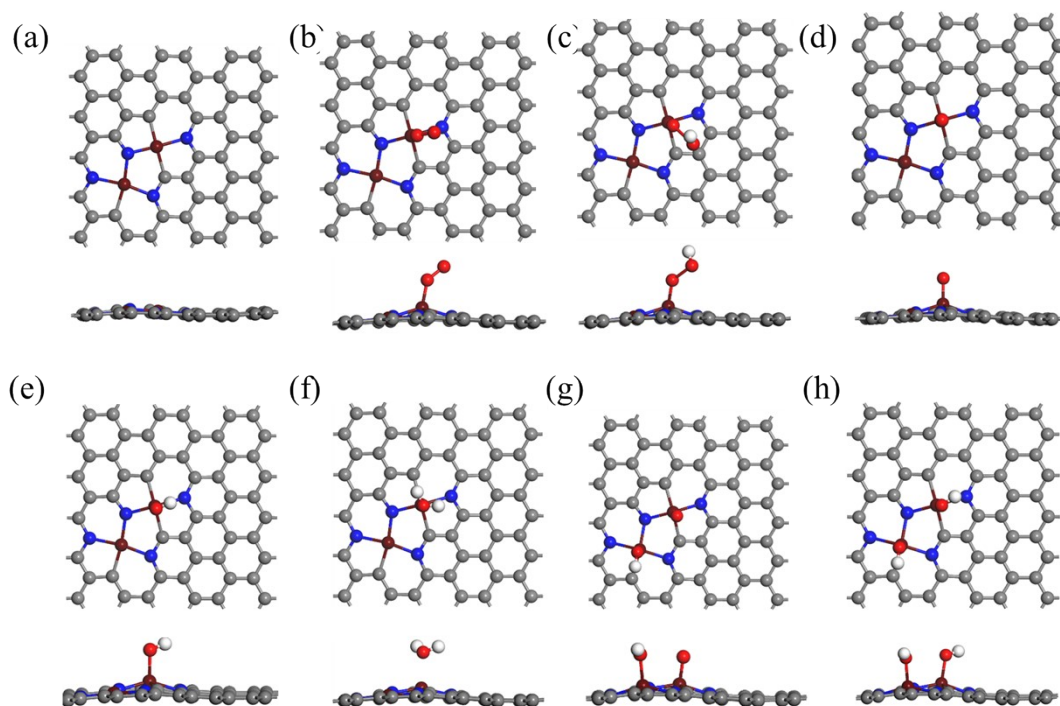==============================================================================



Fig. S15 Optimal structures of the oxygen-containing intermediates adsorbed on $Fe_2N_4$-5-S2/G catalytic surface. (a)*, (b) *$O_2$, (c) *OOH, (d) *O, (e) *OH, (f)$H_2O$*, (g) *O+*OH, (h) *OH+*OH.

Table S1. Bond length (Å) of the oxygen-containing intermediates on these catalysts

| Active site | $O_2$ | | OOH | | O | OH | $H_2O$ | OH+OH | | | O+OH | | |
|---|---|---|---|---|---|---|---|---|---|---|---|---|---|
| | M-O | O-O | M-O | O-O | M-O | M-O | M-O | O-M | O-M | O-O | M-O | M-O | O-O |
| FeN$_2$ | 1.691 | 1.297 | 1.631 | 1.760 | 1.616 | 1.780 | 2.001 | 2.043 | 1.851 | 2.570 | 1.950 | 1.829 | 2.546 |
| 1 | 1.818 | 1.295 | 1.859 | 1.442 | 1.668 | 1.863 | 2.097 | 1.883 | 1.843 | 2.745 | 1.671 | 1.848 | 3.100 |
| 2 | 1.915 | 1.364 | 1.848 | 1.607 | 1.805 | 1.896 | 2.056 | 1.786 | 1.785 | 2.989 | 1.619 | 1.782 | 2.983 |
| 3 | 1.818 | 1.408 | 1.771 | 1.920 | 1.794 | 1.949 | 2.238 | 1.794 | 1.790 | 2.797 | 1.618 | 1.784 | 2.778 |
| 4a-S1 | 1.768 | 1.307 | 1.748 | 1.505 | 1.636 | 1.805 | 2.059 | 1.781 | 1.801 | 3.288 | 1.620 | 1.796 | 3.402 |
| 4a-S2 | 1.743 | 1.311 | 1.745 | 1.513 | 1.637 | 1.806 | 2.043 | 1.781 | 1.801 | 3.288 | 1.780 | 1.625 | 3.369 |
| 4b-S1 | 1.306 | 1.739 | 1.715 | 1.520 | 1.620 | 1.787 | 2.229 | 1.778 | 1.791 | 3.460 | 1.612 | 1.788 | 3.433 |
| 4b-S2 | 1.728 | 1.305 | 1.700 | 1.560 | 1.630 | 1.831 | 2.172 | 1.778 | 1.791 | 3.460 | 1.622 | 1.804 | 3.292 |
| 5a-S1 | 1.787 | 1.297 | 1.811 | 1.463 | 1.641 | 1.868 | 2.267 | 1.855 | 1.826 | 3.484 | 1.639 | 1.815 | 3.438 |
| 5a-S2 | 1.705 | 1.300 | 1.629 | 1.830 | 1.615 | 1.840 | 2.173 | 1.855 | 1.826 | 3.484 | 1.604 | 1.848 | 3.383 |

Table S2. Adsorption energies (eV) of the oxygen-containing intermediates on these catalysts

| Active site | *$O_2$ | *OOH | *O | *OH | *$H_2O$ | Per co-ad *OH |
|---|---|---|---|---|---|---|
| FeN$_2$ | -1.43 | -1.95 | -5.00 | -3.01 | 0.03 | -2.44 |
| 1 | -0.76 | -1.33 | -4.19 | -2.48 | -0.02 | -2.56 |
| 2 | -2.15 | -2.56 | -6.41 | -3.61 | -0.18 | -3.02 |
| 3 | -1.93 | -2.57 | -6.73 | -3.79 | -0.93 | -3.06 |
| 4a-S1 | -1.10 | -1.45 | -4.33 | -2.60 | 0.20 | -2.94 |
| 4a-S2 | -1.40 | -2.02 | -4.58 | -2.63 | -0.36 | -2.94 |
| 4b-S1 | -0.98 | -1.48 | -4.50 | -2.20 | -0.10 | -2.62 |
| 4b-S2 | -1.16 | -1.77 | -4.78 | -2.92 | -0.29 | -2.62 |
| 5a-S1 | -0.71 | -1.18 | -4.19 | -2.49 | -0.16 | -2.68 |
| 5a-S2 | -1.14 | -1.64 | -4.87 | -2.90 | -0.26 | -2.68 |